

Seismic response and retrofitting proposals of the St. Titus Church, Heraklion, Crete, Greece

Michael J. Tzanakis^{1a}, George A. Papagiannopoulos^{2b}
and George D. Hatzigeorgiou^{*3}

¹Engineer Consultant, Ag. Fanouriou 11, GR-71601 Heraklion, Crete, Greece

²Department of Civil Engineering, University of Patras, GR-26500 Patras, Greece

³School of Science and Technology, Hellenic Open University, GR-26335 Patras, Greece

(Received May 26, 2015, Revised March 21, 2016, Accepted April 25, 2016)

Abstract. The purpose of this work is to investigate the seismic behavior of St. Titus Church in Heraklion, Crete, Greece as well as the need of its seismic retrofitting. A numerical model of the Church is constructed using shell finite elements and it is then seismically examined using response spectrum and linear time-history analyses. Effects of soil-structure interaction have been also taken into account. The Church without retrofit is expected to exhibit extensive tensile failures and many compressive ones. Aiming to maintain the architectural character of the structure as well as to increase its seismic resistance, a retrofitting procedure involving injection of cement grout in conjunction with reinforced concrete jacketing to the internal side of the masonry walls is proposed. A numerical implementation of the proposed seismic retrofitting is performed and its effect is evaluated by response spectrum and linear time-history analyses. From the results of these analyses, it is shown that compressive failures are eliminated while only few tensile failures of local character take place.

Keywords: seismic response; masonry; retrofitting; response spectrum; time-history

1. Introduction

Preservation of a historical monument involves multidisciplinary considerations and cannot have as only aim its survival. Strengthening of a historical monument should aim to keep its aesthetics, character as well as its architectural value. Taking into account that the behavior of historical monuments is generally more complex than that of modern ones, application of current analysis methods in order to evaluate their behavior may lead to incomplete, crude or even erroneous results. Therefore, knowledge of the mechanical characteristics of the structural elements of a historical monument is necessary for reliable static analysis (Kržan *et al.* 2015). To this point, one should also mention the role of experimental techniques and of monitoring using non-destructive procedures (Roca *et al.* 1997).

*Corresponding author, Associate Professor, E-mail: hatzigeorgiou@eap.gr

^aMSc., E-mail: miktzan@yahoo.com

^bPh.D., Lecturer, E-mail: gpagapia@upatras.gr

On the other hand, even if extensive knowledge of the monument is available, its past history cannot be disregarded. In fact, it is also important to collect data about the construction techniques used, including subsequent reinforcement or restoration works. These past history data may offer valuable information when interpreting the static behavior of the monument and when defining additional investigations to be undertaken (Roca *et al.* 1997).

The numerical structural analysis of a historic monument requires the elaboration of a structural model on the basis of the geometry of the monument and the characteristics of its material. Most historical monuments are built from masonry, a building material that inevitably includes a large number of possible combinations generated by the geometry and arrangement of units such as bricks, blocks, ashlars as well as their joining using mortar. Irrespective of their arrangement, masonry units have one common feature, i.e., their very low tensile strength. Thus, masonry easily develops cracking under intense seismic actions.

Masonry essentially exhibits anisotropic behavior and its real stress-strain relationship is non-linear. Thus, a non-linear analysis (e.g., Betti and Galano 2012) in conjunction with a probabilistic vulnerability assessment (e.g., Pagnini *et al.* 2012) should be more suitable for seismic response purposes. However, for the case of unreinforced masonry which exhibits brittle behavior, non-linear analysis may not always lead to reliable response results due to significant uncertainties in material response (Roca *et al.* 1997, Bull 2001). Therefore, linear analysis considering isotropic behavior may be preferable because it can provide a useful picture of the overall stress state (mainly stress concentration) and identify critical regions that deserve more accurate study (Meli and Peña 2004, Betti *et al.* 2010). Additionally, linear elastic analysis is quite useful since it can provide with very important results about the natural modes of vibration and their corresponding frequencies. Furthermore, linear analysis can be preferred in comparison with non-linear analysis if the main objective is to compare the behavior of the strengthened structure with that of the unstrengthened structure (Triantafillou and Fardis 1997). On the other hand, provided that structural details are realistically idealized and calibrated into the analysis model, linear analysis and the interpretation of its results may constitute a guideline for choosing more refined material models as those described in Roca *et al.* (1997) and Bull (2001). In general, the analysis of a monumental structure can be performed by using finite and/or boundary elements (Beskos 1993, 1994).

The Church of St. Titus is considered one of the most important historical monuments in Heraklion, Crete, Greece. The frequent occurrence of earthquakes there, as well as in the surrounding region, constitutes a convincing argument of the seismic risk that this monument is subjected to. In order to obtain an estimate of this seismic risk, it is desirable to perform several numerical analyses of the structure on the basis of all available data that would help towards this direction. These analyses have been decided to be as simple as possible taking into account that the material of the Church is unreinforced masonry. Thus, only linear analyses by using both response spectrum and time integration techniques have been conducted, in order to get a preliminary seismic response assessment of the structure under consideration.

From the results of these linear analyses, it is concluded that extensive tensile cracks may appear at the Church and, thus, a retrofitting procedure has to be proposed. This retrofitting procedure is also supported by linear analyses. It has been found that a combination of mass impregnation in conjunction with reinforced concrete jacketing to the internal side of the masonry walls significantly improves the seismic behavior of the Church as the tensile failures may be drastically reduced. The effect of soil-structure interaction (SSI) has also been studied for both the non-retrofitted and retrofitted structure.

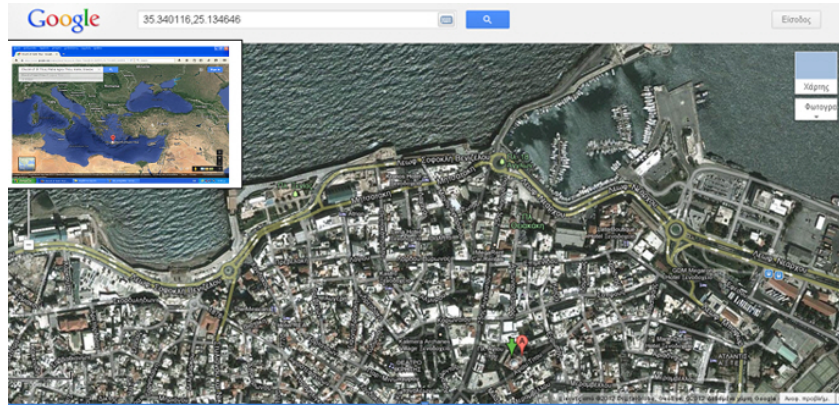


Fig. 3 Position of St. Titus Church

The vestibule has dimensions 23.35×7.20 m and it is located at the north-west side of the main temple. It was built together with the main temple although some minor conversions were performed later. Its roof is made of reinforced concrete, substituting a former wooden roof. Moreover, an additional reinforced concrete slab having a thickness of 14 cm, supported by perimeter and lateral beams having height-to-width dimensions in cm 50×25 and 25×64 , respectively, was constructed inside the vestibule. An excavation at 2.90 m depth took part under the vestibule in order to create a basement used for storing purposes. A reinforced concrete slab of a thickness of 17 cm, supported by lateral beams having height-to-width dimensions in cm 30×67 , was used to cover the basement. Regarding the foundation, it is believed that it is same for all parts of the Church, i.e., at a depth of 2.90 m which was obtained during the aforementioned excavation.

Indicative architectural drawings of the Church, originally imprinted, are shown in Figs. 4 and 5.

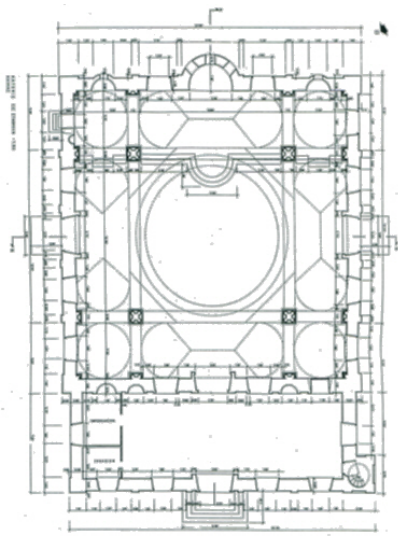


Fig. 4 Floor plan of St. Titus Church

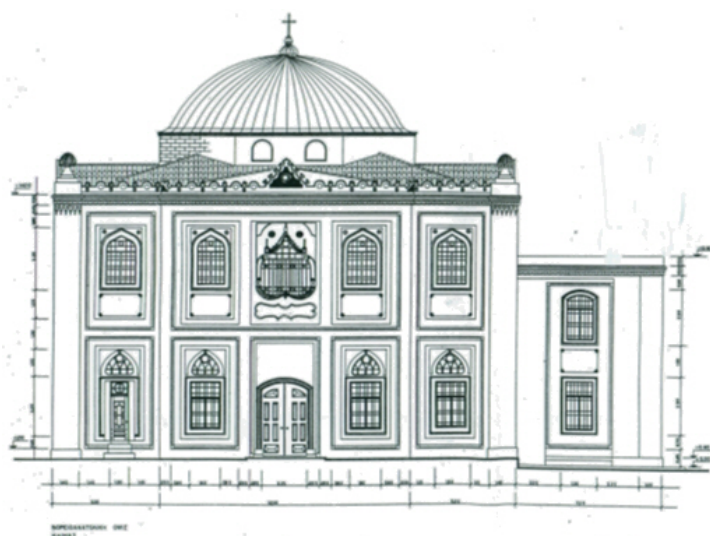


Fig. 5 External side of St. Titus Church

2.3 Damage state

Damages in the form of cracks have been exhibited due to both the frequent occurrence of weak-to-moderate earthquakes and to the oxidization of the anchored parts of the steel tie rods at the external walls. These cracks have been imprinted in detail at the beginnings of 1970 and are indicatively, shown in Figs. 6-8.

Restoration works performed between 1974-1977 were focused mainly on filling of cracks, reconstruction of parts of masonry walls and replacement of vertical steel anchors of tie rods. Extensive horizontal and vertical cracks were also reported in 1985 especially at the north-east side of the Church. Additional restoration works took place after 1985 and included cement injections, replacement of steel anchors as well as of wooden parts at the dome etc.

In 2001, an inspection for damage due to the seismic activity, conducted under the initiative of local authorities, revealed extensive horizontal cracks close to the edges of several windows, vertical cracks at the top of external walls, a few skewed cracks at both the internal and the

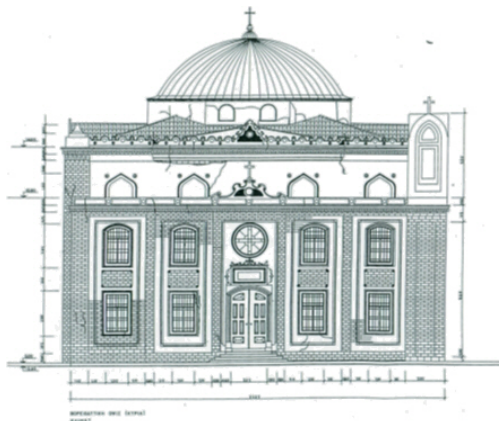


Fig. 6 Cracks at the external side of St. Titus Church

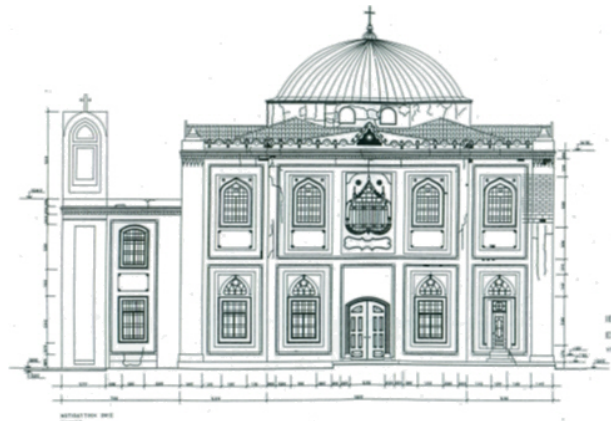


Fig. 7 Cracks at the external side of St. Titus Church

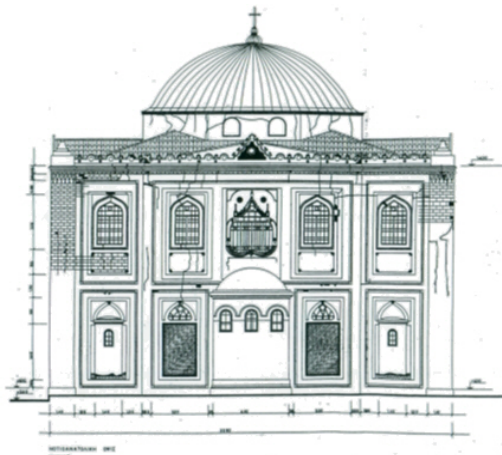


Fig. 8 Cracks at the external side of St. Titus Church



Fig. 9 Current status, oxidization at south-east side Fig. 10 Current status, oxidization at south-west side

external sides of masonry as well as severe oxidization of the anchored parts. Similar cracks were identified by the authors of the present paper during their visits at the Church between 2010-2013 and are indicatively shown in Figs. 9 and 10. The internal part of the structure is in good condition and no visible cracks exist. Soil settlements have not been observed.

On the basis of the previously presented damage state, it has been considered important a) to eliminate the danger for the pedestrians due to falls of stone parts around the Church (as a result of the oxidization of the anchored parts and of the effect of weak earthquakes) and b) to study how to protect the monument from possible partial collapse in the case of a strong earthquake.

3. Materials and numerical model

The restoration works performed up to now have been based only on visible damages and not on a numerical simulation of the static and dynamic behavior of the Church. Thus, it is reasonable to claim that a more successful restoration attempt should include data coming from detailed finite element analyses of the Church. These analyses would highlight the most vulnerable parts of the Church especially in the case of an intense earthquake. In the following, the material data needed to perform these analyses as well as the numerical model of the Church as presented.

3.1 Materials

The masonry walls of the Church were made from local limestone and they also include an external leaf in the facade of 20 cm made of ashlar. The mortars of both external walls and internal coatings have a limestone basis, whereas the ashlars have been constructed in contact and grouting exists among their joints. The external walls have a thickness of 0.95 m, slightly differing at the niches, and of 1.05 m between the main temple and the vestibule.

In absence of any in-situ or laboratory data for the material of the structure under study, the mechanical properties of the masonry considered for the analyses have been estimated using the masonry synthesis results coming from a similar monument in Heraklion, the Pantokrator Gate,

where a detailed investigation has been performed (Arvanitaki and Voyadjis 2012).

In order to take into account the uncertainties inherent in the values of the masonry properties, three values acting as upper, mean and lower values for the compressive strength of the masonry have been considered. These values are 20.14 MPa, 13.10 MPa and 7.32 MPa, respectively, and come from the results of masonry synthesis of the Pantokrator Gate (Arvanitaki and Voyadjis 2012). The compressive strength of the mortar, f_{mc} , based on values recommended from various researches in other similar works, has been taken equal to 1.08 MPa. The specific weight of the unreinforced masonry and its Poisson ratio has been considered to be 20 KN/m³ and 0.2, respectively.

Table 1 provides the compressive strength, the characteristic compressive strength, the elasticity and shear moduli and the maximum tensile strength of the unreinforced masonry (Bull 2001, EC 6 2009). This maximum tensile strength, f_{wt} , has been calculated on the basis of the compressive strength of the mortar f_{mc} as

$$f_{wt} = \lambda \cdot 1/4 \cdot \sqrt{f_{mc}} \tag{1}$$

where $\lambda=0.7$ and $f_{mc}=1.08$ MPa. Thus, the maximum tensile strength is 0.18 MPa and is in accordance with the experimental values of tensile strength given in Tomažević (1999). Depending on the strength of the bricks for each case considered, the shear strength of the masonry, f_{vk} , has been found equal to 0.20-0.30 MPa, employing the following requirement (EC6 2009)

$$f_{vk} = 0.7 \cdot \min [f_{vko} + 0.4\sigma_d, \max(0.065f_b, f_{vlt})] \tag{2}$$

where f_{vk} is the characteristic initial shear strength under zero compressive stress, σ_d is the design compressive stress perpendicular to the shear in the member at the level under consideration, f_b is the normalized compressive strength of the masonry units, f_{vlt} is a limit to the value of f_{vk} .

According to the findings of a previous investigation made for the Church under study (Vasilakis *et al.* 1979), the values of the mechanical properties of wood for its arched members as well as for those members that form its dome are considered to be as follows: specific weight is 3.4 KN/m³, modulus of elasticity is 6.7 GPa, Poisson ratio is 0.3, tensile strength is 13 MPa and compressive strength is 20 MPa. These strengths are based on wood grains that run essentially parallel to the length of the members. Thus, the dome is considered to form a diaphragm of a thickness of 25 cm and to behave isotropically on the basis of the aforementioned values for its mechanical properties.

Regarding the newer concrete beams and slab constructions at the vestibule, the values considered for specific weight, modulus of elasticity, Poisson ratio, compressive and tensile strength are 25 KN/m³, 28 GPa, 0.2, 18 MPa and 1.8 MPa, respectively. Due to cracking, 35% of

Table 1 Properties of the masonry considered for the analyses

	Compressive strength (MPa)	Characteristic compressive strength (MPa)	Modulus of elasticity (GPa)	Shear modulus (GPa)	Maximum tensile strength (MPa)
Upper	20.14	3.59	3.59	1.50	0.18
Medium	13.10	2.71	2.71	1.13	0.18
Lower	7.32	1.86	1.86	0.78	0.18

the gross stiffness has been taken into account. Regarding the steel reinforcement of the concrete beams and the slab, the specific weight, modulus of elasticity, Poisson ratio and yield strength have been considered with the values 78.5 KN/m^3 , 200 GPa, 0.3 and 400 MPa, respectively. Similarly, steel truss rods are considered to be of S235 steel, thus, the only difference with the previously mentioned values is that of the yield strength which now is 235 MPa.

3.2 Numerical model

On the basis of the architectural drawings available, a numerical model of the Church using finite elements is implemented in SAP 2000 (2010). Masonry columns, steel truss rods, reinforced concrete beams and arched wood members have been modeled by beam-column elements, whereas the masonry walls, the wooden dome and the reinforced concrete slab by using shell elements having the thicknesses mentioned in a previous section. The doors and windows have been also taken into account.

The structure is initially considered to be fixed at its base, i.e., having no interaction with soil. Then, to take into account possible SSI effects, the Church is considered to be founded on a soil type of class C according to EC8 (2009) using discrete mass-stiffness-dashpot elements. The numerical properties of these discrete elements, i.e., mass, stiffness and damping have been quantified on the basis of the approach presented in Mulliken and Karabalis (1998).

The selection of a C class type of soil (EC8 2009) is compatible with the available geotechnical data for the region under study. Thus, the shear wave velocity, the mass density and the Poisson ratio of the soil have the following values: 270 m/sec, 2000 kgr/m^3 and 0.3, respectively. In order to take into account the inelastic behavior of the soil, its shear modulus is considered to be 40% of its initial value one calculated on the basis of the aforementioned values for shear wave velocity and density. The basement under the vestibule, mentioned in section 2.2, has been ignored in all SSI analyses.

4. Seismic response results and retrofitting techniques

The seismic response analyses performed in this section aim to reveal the more stressed parts of the Church and to highlight the need of its retrofit. The seismic response of the structure is obtained by using response spectrum and linear time-history analyses. Retrofitting of the Church is also supported by these types of analyses. Linear analysis can be preferred in comparison with non-linear analysis if the main objective is to compare the behavior of the strengthened structure with that of the unstrengthened structure (Triantafyllou and Fardis 1997). Moreover, linear analyses considering isotropic behavior can provide a useful picture of the overall stress state (mainly regions with stress concentration) and identify critical regions that deserve more accurate study (Meli and Peña 2004, Betti *et al.* 2010). In order to evaluate the probable damage state, the principal stresses (F_{11} and F_{22} , according to SAP 2000 terminology) are examined. Regarding the results of the analyses presented in the following, it has been considered that tensile failure occurs when the computed tensile stresses exceed the maximum assumed tensile strength.

4.1 Response spectrum analyses

Modal analysis revealed that at least 200 modes are needed to obtain participation of modal

mass greater than 90% in both horizontal direction X and Y of the Church. Figs. 11 and 12 show the first two periods of the fixed-base Church in X and Y direction, respectively, for the case of 1.86 GPa, which is the lowest modulus of elasticity assumed for masonry. The periods are found approximately equal to 0.27 sec and 0.21 sec and their corresponding mass participation is 50.5% and 64.3%, respectively. For the same value of the modulus of elasticity, Figs. 13 and 14 show the first two periods of the Church considering SSI effects. The periods found are approximately equal to 0.32 sec and 0.27 sec and their corresponding mass participation is 54.7% and 58.6%, respectively. The mode shapes of Figs. 11-14 exhibit an almost translational character.

Similar results regarding periods and participation of modal mass have been obtained for the other two values of the modulus of elasticity given in Table 1. It should be noted that fewer modes were needed to obtain participation of modal mass greater than 90% in both horizontal direction X and Y of the Church when SSI effects are considered. The results of modal analyses for all cases



Fig. 11 First mode of the Church in X direction



Fig. 12 First mode of the Church in Y direction

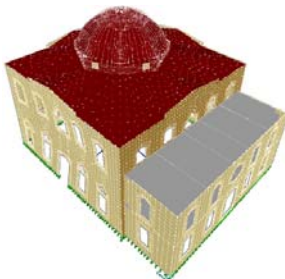


Fig. 13 First mode of the Church in X direction considering SSI effects



Fig. 14 First mode of the Church in Y direction considering SSI effects

Table 2 Results of modal analyses

Modulus of elasticity (GPa)	Model	1 st modal period (sec) - X direction	1 st modal period (sec) - Y direction	% total modal mass for 200 modes - X direction	% total modal mass for 200 modes - Y direction
1.86	Fixed	0.2726	0.2123	90.22	90.74
1.86	SSI	0.3256	0.2740	97.06	96.72
2.71	Fixed	0.2313	0.1797	89.93	90.49
2.71	SSI	0.2832	0.2438	98.27	97.92
3.59	Fixed	0.2047	0.1589	89.71	90.27
3.59	SSI	0.2555	0.2237	98.54	98.47

examined are shown in Table 2. As expected, from the results of Table 2, the fundamental periods of the Church for both horizontal directions increase when considering SSI effects in comparison to their fixed-base values.

Stress results have been obtained by the sum of gravity and seismic loads following Eurocode 8 (2009), whereas the CQC method has been used for modal synthesis purposes. The peak ground acceleration used was 0.24 g, multiplied by 1.4 due the importance of the structure. Two values of modal damping ratios, i.e., 4% and 7% (Elmenschawi *et al.* 2010), have been employed by means of the damping modification factor of Eurocode 8 (2009).

Tensile and compressive normal stresses for the three values of modulus of elasticity of Table 1 and the two values of modal damping ratios, i.e., 4% and 7% are computed. Figs. 15-17 have been obtained using a modulus of elasticity equal to 1.86 GPa and a modal damping ratio equal to 7%. These figures show the horizontal tensile normal stresses and the vertical compressive and tensile normal stresses at the front view of the Church considering it as fixed-base. Similar stress plots are given in Figs. 18-20 using the same values for modulus of elasticity and modal damping ratio but considering now SSI effects.

From the results of Figs. 15-20, it is concluded that the seismic combinations mandated by Eurocode 8 (2009) may lead to extensive tensile failures at all sides of the structure, while compressive failures also take place around the central openings at the north, south and east sides of the Church, using as orientation the sides of Fig. 4. These failures are in accordance with the damage observed to the external sides of the Church before its restoration in the decade 1970-1980 (described in section 2.3) as well as with the present damage state of the external sides.

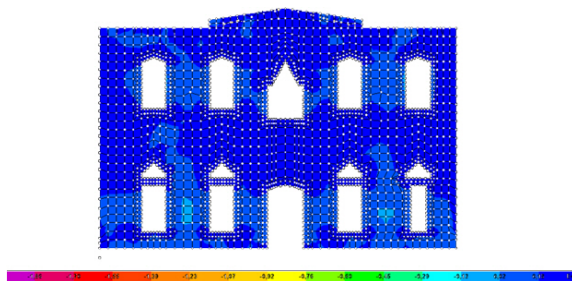


Fig. 15 Horizontal tensile normal stresses (in MPa) at the front view of the fixed-base Church

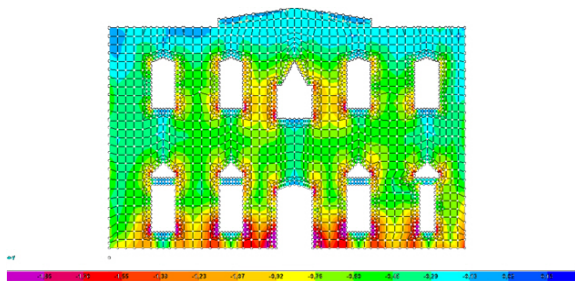


Fig. 16 Vertical compressive normal stresses (in MPa) at the front view of the fixed-base Church

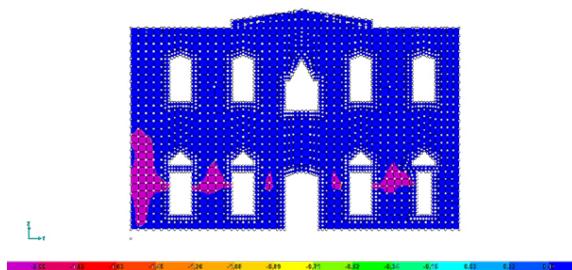


Fig. 17 Vertical tensile normal stresses (in MPa) at the front view of the fixed-base Church

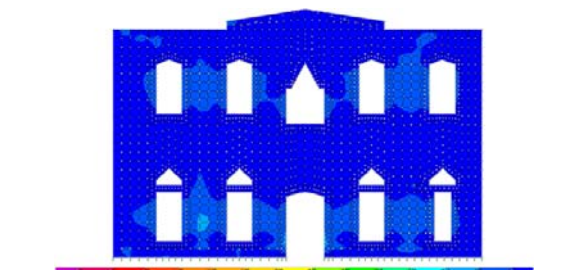


Fig. 18 Horizontal tensile normal stresses (in MPa) at the front view of the Church considering SSI effects

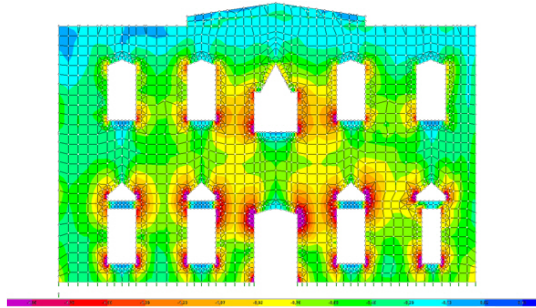


Fig. 19 Vertical compressive normal stresses (in MPa) at the front view of the Church considering SSI effects

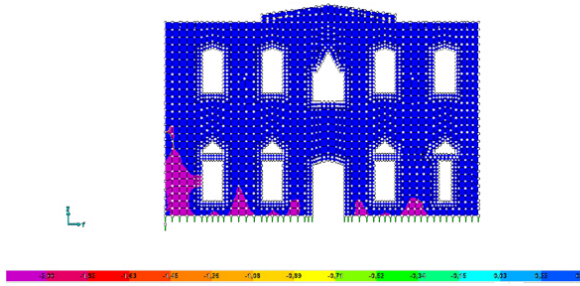


Fig. 20 Vertical tensile normal stresses (in MPa) at the front view of the Church considering SSI effects

Employing the rest combinations between the modulus of elasticity and modal damping ratio values, similar results regarding tensile failures have been found, whereas regarding the compressive failures there is an improvement as modulus of elasticity increases. More specifically, compressive failures are almost absent for the case of modulus of elasticity and modal damping ratio equal to 3.59 GPa and 7%, respectively. This absence of compressive failures is mainly justified by the stiffening of the material and its increased compressive strength. The dominant natural periods of the Church in both directions have been decreased but they are not less than the value of the corner period T_B of the spectrum considered (Eurocode 8 2009).

4.2 Retrofitting using response spectrum analyses

In this section two retrofitting techniques are employed in order to increase the seismic resistance of the Church, i.e., mass impregnation and reinforced concrete jacketing. The implementation of these two techniques is performed by adjusting the properties of the masonry and it is described in what follows. It should be noted that both retrofitting techniques keep the architectural character of the Church. Since only linear analyses are employed herein and failure is considered to take place when tensile strength is exceeded, the aim of the proposed two retrofitting techniques is to effectively reduce tensile stresses by retardation of the occurrence of the tensile failures.

The technique of mass impregnation involves injection of a cement grout in order to fill cracks or voids in the masonry. It usually offers significant improvement to the compressive strength of masonry especially when the mortar is of low quality and has low strength. The compressive strength of masonry increases using the empirical relationship of Tomažević and Apih (1993)

$$f_{wc,s} = f_{wc,0} [1 + 0.013(100G_{gr}/G_0)]^3 \quad (3)$$

using a volume ratio G_{gr}/G_0 equal to 6%, where G_{gr} is the volume of the grout injected in a masonry of volume G_0 . For grouts having compressive strength of 10 MPa, the tensile strength of masonry is taken as 10% of the compression one. The use of a special cement grout which contains either white cement, pozzolan and lime paste is suggested. This cement grout can provide the necessary strength which is indeed very close to the strength of the original mortar used. The viscosity of the cement grout can be adjusted in order to fill the voids of the masonry (the external leaf has 20 cm thick and is made by squared ashlar placed in direct contact), using an appropriate

pressure (about 6 bars).

In view of the aforementioned considerations, the modified properties of masonry are given in Table 3. Modal analyses results for the retrofitted Church are given in Table 4. For the case of the lower modulus of elasticity of Table 3, i.e., 7.08 GPa, the first two periods of the fixed-base Church are approximately equal to 0.16 sec and 0.12 sec and their corresponding mass participation is 47.2% and 51.8%, respectively.

For the three new values of modulus of elasticity of Table 3 and the two values of modal damping ratio, i.e., 4% and 7%, the maximum compressive and tensile normal stresses are computed, considering the building either fixed-base or with SSI effects. From the results obtained by spectrum analyses, it is found that the retrofitted Church still exhibits numerous tensile failures at all of its sides, while compressive failures do not exist. This reveals the effectiveness of the retrofitting technique even for the case of the minimum values for modulus of elasticity and modal damping ratio considered, i.e., 7.08 GPa and 4%, respectively. As modulus of elasticity increases, tensile failures become less but they are not eliminated.

Aiming to improve the situation, the retrofitting process continues with the addition of reinforced concrete jackets in conjunction with mass impregnation. These jackets are usually constructed on both sides of a masonry wall (Modena *et al.* 1997, Penazzi *et al.* 2001) but may also be applied on only one side. A successful application of this one-sided jacketing can be found in Arède *et al.* (2012). In order to preserve the character of the external sides of the peripheral masonry walls, a one-sided jacket having a thickness of 10 cm is constructed on the internal side of the peripheral masonry walls of the Church. On the other hand, a two-sided jacket having a thickness of 5 cm at each side can be constructed at the masonry walls between the main temple and the vestibule. The proposed jacketing procedure is considered to be efficient from both constructional and economical points of view.

To simulate the reinforced concrete jackets in the numerical model, the ‘shell section layer’

Table 3 Properties of the masonry considering injection of cement grout

	Initial modulus of elasticity (GPa)	Characteristic compressive strength (MPa)	Compressive strength (MPa)	New modulus of elasticity (GPa)	Maximum tensile strength (MPa)
Upper	3.59	3.59	13.67	13.67	1.37
Medium	2.71	2.71	10.32	10.32	1.03
Lower	1.86	1.86	7.08	7.08	0.71

Table 4 Results of modal analyses for the retrofitted Church by using mass impregnation

Modulus of elasticity (GPa)	Model	1 st modal period (sec) - X direction	1 st modal period (sec) - Y direction	% total modal mass for 200 modes - X direction	% total modal mass for 200 modes - Y direction
7.08	Fixed	0.1578	0.1229	89.14	89.59
7.08	SSI	0.2075	0.1875	99.40	99.33
10.32	Fixed	0.1357	0.1063	88.78	89.02
10.32	SSI	0.1847	0.1686	99.20	99.15
13.67	Fixed	0.1219	0.0965	88.56	88.35
13.67	SSI	0.1701	0.1559	99.66	99.69

Table 5 Results of modal analyses for the retrofitted Church by using mass impregnation and reinforced concrete jackets

Modulus of elasticity (GPa)	Model	1 st modal period (sec) - X direction	1 st modal period (sec) - Y direction	% total modal mass for 200 modes - X direction	% total modal mass for 200 modes - Y direction
7.08	Fixed	0.1341	0.1096	88.76	88.85
7.08	SSI	0.1899	0.1727	99.74	99.73
10.32	Fixed	0.1217	0.0994	88.48	88.36
10.32	SSI	0.1754	0.1602	99.77	99.78
13.67	Fixed	0.1131	0.0925	88.43	88.00
13.67	SSI	0.1663	0.1524	99.79	99.81

option of SAP 2000 (2010) is adopted. Using this option, a section is defined on the basis of two layers having different thickness and different material properties, while perfect bonding between the layers is assumed. Modal analyses results for the retrofitted, by using mass impregnation and reinforced concrete jackets, Church are given in Table 5. For the case of the lower modulus of elasticity of Table 5, i.e., 7.08 GPa, the first two periods of the fixed-base building are approximately equal to 0.13 sec and 0.11 sec and their corresponding mass participation is 53.3% and 51.0%, respectively.

Maximum compressive and tensile normal stresses for the three new values of modulus of elasticity of Table 5 and the two values of modal damping ratio, i.e., 4% and 7% are computed, considering the retrofitted Church either fixed-base or with SSI effects. Figs. 21 and 22 have been obtained using modulus of elasticity equal to 7.08 GPa and modal damping ratio equal to 4% and show the tensile normal stresses at the front view of the fixed-base Church and at the wall between the main temple and the vestibule, respectively. Similar results are obtained for the aforementioned values of modulus of elasticity and damping ratio considering the Church with SSI effects. From the stresses shown in Figs. 21 and 22, as well from the rest of the cases studied, it has been found that tensile failures exhibit a local character at the external sides of the peripheral walls.

Figs. 23 and 24 display the compressive and tensile normal stresses at the front view of the retrofitted Church considering it to be fixed-base. It has been found that the maximum compressive and tensile stresses are -5.60 MPa and 2.70 MPa, respectively. The maximum compressive stress is much less than that of a typical reinforced concrete having a strength of 20 MPa. The maximum tensile stress has to be explicitly delivered by steel reinforcement. Simple calculation per meter length and for a thickness of 10 cm of the jacket, leads to steel reinforcement $\Phi 12/12.5$ cm, where the strength of steel is 400 MPa. Figs. 25 and 26 show the minimum and maximum, respectively, shear stresses along the interface between the masonry wall and the jacket, in order to estimate the diameter of the anchors needed. It was found that the minimum and maximum compressive and shear stresses are -0.80 MPa and 0.80 MPa, respectively. Simple calculations lead to $\Phi 18/12.5$ cm anchors placed in grid.

Up to here, the previously presented results regarding tensile stresses are considered to represent the worst case scenario in terms of expected seismic response. For modulus of elasticity equal to 10.32 or 13.67 GPa, these tensile stresses are effectively reduced. Increasing modal damping from 4% to 7%, does not lead to further reductions in tensile stresses. The same trends regarding stresses hold either the Church is fixed on its base or with SSI effects considered.

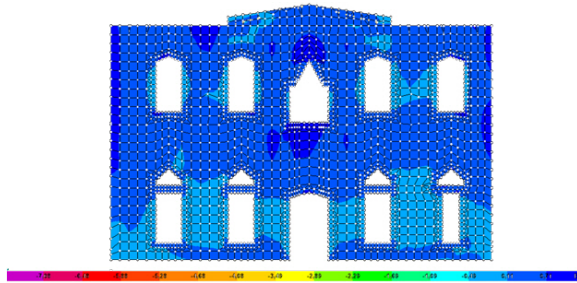


Fig. 21 Tensile normal stresses (in MPa) at the front view of the fixed-base Church

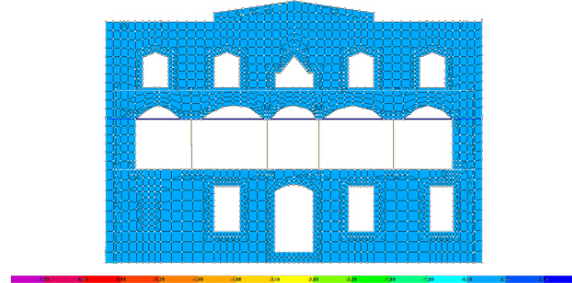


Fig. 22 Tensile normal stresses (in MPa) at the wall between the main temple and the vestibule of the fixed-base Church

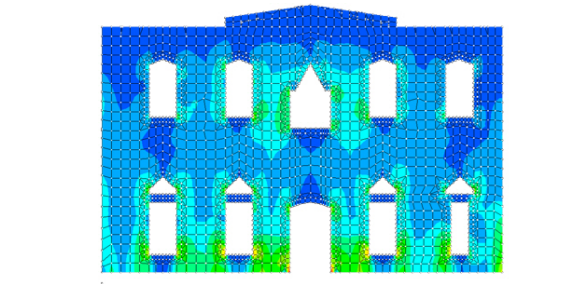


Fig. 23 Compressive normal stresses (in MPa) at the front view of the retrofitted fixed-base Church

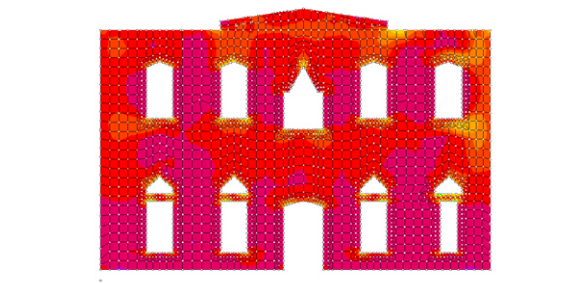


Fig. 24 Tensile normal stresses (in MPa) at the front view of the retrofitted fixed-base Church

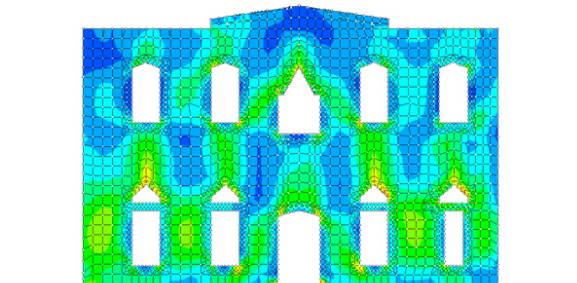


Fig. 25 Minimum shear stresses (in MPa) at the front view of the retrofitted fixed-base Church

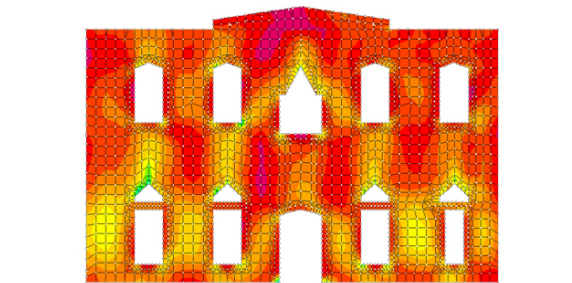


Fig. 26 Maximum shear stresses (in MPa) at the front view of the retrofitted fixed-base Church

4.3 Time-history analyses

In this section, stress results by using linear time-history analyses are presented. All plots that follow are shown up to the time initiation of tensile or compressive failures.

The selection of recorded accelerograms for performing time-history analyses is based on the restrictions posed by Eurocode 8 (2009) as well as on the available seismic hazard studies for the broader area of the island of Crete, e.g., Tsapanos (2003). These accelerograms correspond to earthquakes of magnitude greater than 7.0, which is in accordance with the macroseismic data provided by Papazachos and Papazachou (2004) and the existence of extended offshore faults in

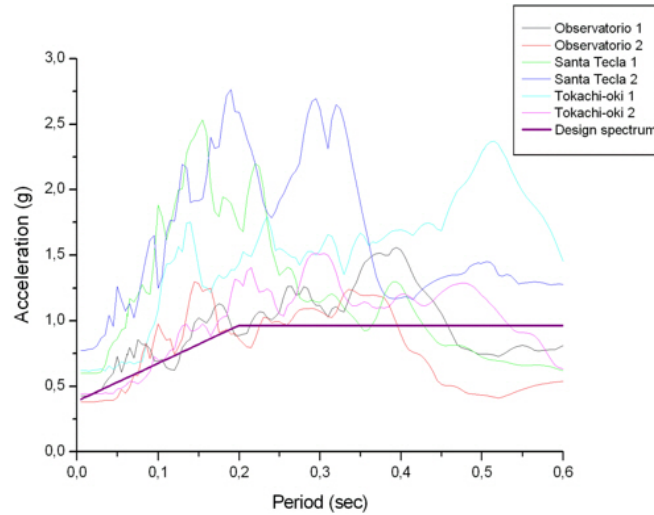


Fig. 27 Response spectra of the accelerograms used

the broader area. The three accelerograms which were eventually selected are a) the Observatorio and Santa Tecla recordings from the 13/1/2001 San Salvador earthquake and b) the HKD092 recording from the 25/9/2003 Tokachi-Oki, Japan earthquake. These accelerograms have been downloaded from COSMOS (1999). The response spectra of the two horizontal components for each one of the aforementioned three accelerograms and for the period range of 0.005 to 0.6 sec are given in Fig. 27. In the same figure, the reference design spectrum is also given.

The results for the non-retrofitted Church are presented first. Considering the case of modulus of elasticity equal to 1.86 GPa and modal damping ratio equal to 4%, Figs. 28 and 29 display the distribution of horizontal and vertical normal stresses, respectively, for the case of the Observatorio strong ground motion accelerogram. It has been concluded that on a qualitative basis, the results obtained previously by spectrum analyses are verified. Extensive tensile failures take place at all peripheral walls of the Church, while compressive failures appear at the region of the central openings. Maximum compressive and tensile stresses are -5.16 MPa and 3.31 MPa, respectively, surpassing about 2.77% and 17.53% the corresponding ones coming from spectrum analyses.

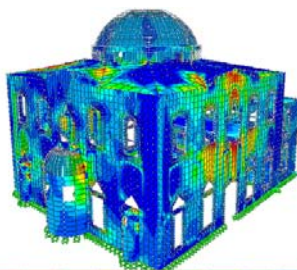


Fig. 28 Horizontal normal stresses (in MPa) for the case of Observatorio strong ground motion accelerogram

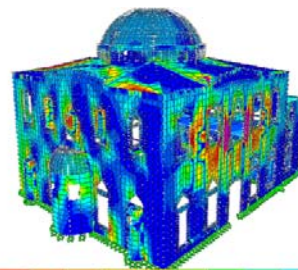


Fig. 29 Vertical normal stresses (in MPa) for the case of Observatorio strong ground motion accelerogram

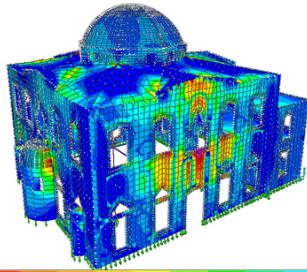


Fig. 30 Horizontal normal stresses (in MPa) for the case of Observatorio strong ground motion accelerogram considering SSI effects

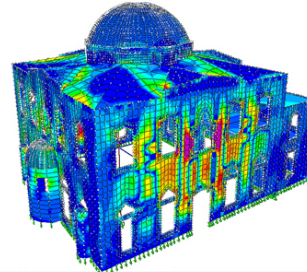


Fig. 31 Vertical normal stresses (in MPa) for the case of Observatorio strong ground motion accelerogram considering SSI effects

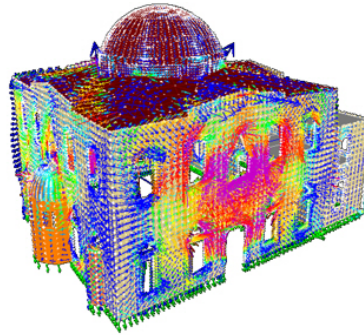


Fig. 32 Direction of stresses for the case of the fixed-base Church subjected to Observatorio strong ground motion accelerogram

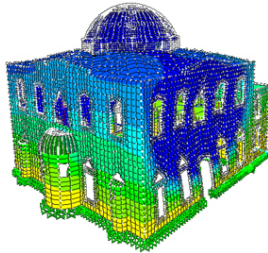


Fig. 33 Horizontal displacements along the X direction of the fixed-base Church for the case of Observatorio strong ground motion accelerogram

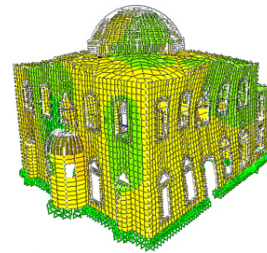


Fig. 34 Horizontal displacements along the Y direction of the fixed-base Church for the case of Observatorio strong ground motion accelerogram

Similar results have been obtained for the cases of the other two accelerograms as well as for all cases when SSI effects are taken into account. Regarding the influence of SSI effects, Figs. 30 and 31 show the distribution of horizontal and vertical normal stresses, respectively, up to the critical point of linear elastic response for the case of the Observatorio strong ground motion accelerogram, modulus of elasticity equal to 13.67 GPa and damping ratio equal to 4%. To get an idea of the direction of total stresses, Fig. 32 is provided for interpretation purposes of the stress results of Figs. 30 and 31.

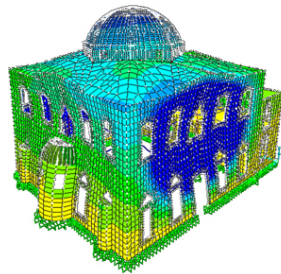


Fig. 35 Horizontal displacements along the X direction of the fixed-base Church for the case of Santa Tecla strong ground motion accelerogram

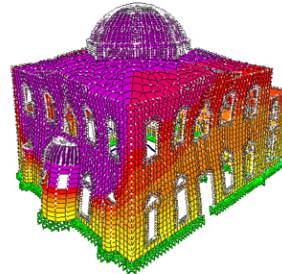


Fig. 36 Horizontal displacements along the Y direction of the fixed-base Church for the case of Santa Tecla strong ground motion accelerogram

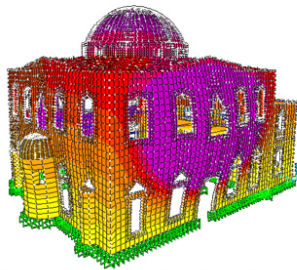


Fig. 37 Horizontal displacements along the X direction of the fixed-base Church for the case of Tokachi-Oki strong ground motion accelerogram

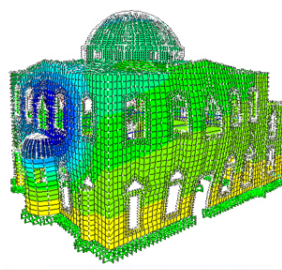


Fig. 38 Horizontal displacements along the Y direction of the fixed-base Church for the case of Tokachi-Oki strong ground motion accelerogram

For comparison purposes, Figs. 33-38 show the horizontal displacements at X and Y directions of the fixed-base Church when it is subjected to the aforementioned three accelerograms.

4.4 Retrofitting using time-history analyses

Stress results coming from time-history analyses of the retrofitted Church are expected to verify the efficiency of the combination of mass impregnation and reinforced concrete jacketing in reducing drastically the tensile failures. The efficiency of this combination has been also proven previously by response spectrum analyses.

The effect of application of only mass impregnation is depicted first. Considering again the case of modulus of elasticity equal to 7.08 GPa and damping ratio equal to 4%, Figs. 39 and 40 show the distribution of horizontal and vertical normal stresses, respectively, for the case of the Obesrvatorio strong ground motion accelerogram. The retrofitted fixed-based structure does not exhibit any compressive failures, however, some tensile failures due to horizontal stresses occur. Similar results are obtained for the cases of the other two accelerograms as well as for all cases when SSI effects are taken into account. As modulus of elasticity increases to 13.67 GPa, tensile failures become less but they are not eliminated.

It has been verified that among the accelerograms used for performing time-history analyses for both the non-retrofitted and the retrofitted Church, the Santa Tecla one lead to more failures in comparison to other two. For this reason, the effect of employing reinforced concrete jackets in

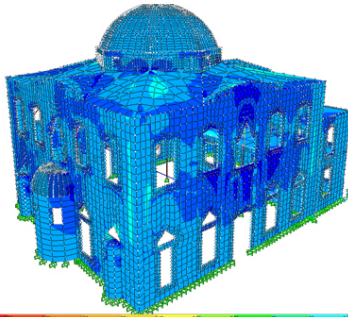


Fig. 39 Horizontal normal stresses (in MPa) for the retrofitted Church by applying mass impregnation, subjected to Observatorio strong ground motion accelerogram

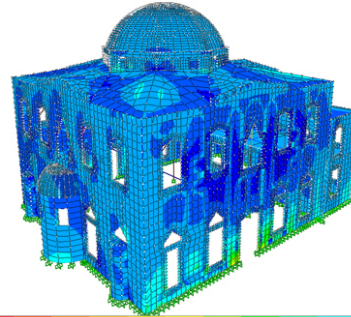


Fig. 40 Vertical normal stresses (in MPa) for the retrofitted Church by applying mass impregnation, subjected to Observatorio strong ground motion accelerogram

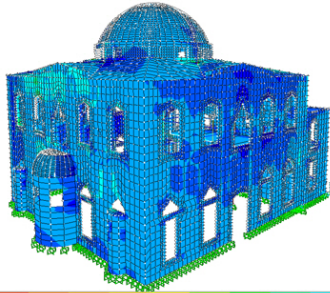


Fig. 41 Horizontal normal stresses (in MPa) for the retrofitted Church by applying mass impregnation, subjected to Santa Tecla strong ground motion accelerogram

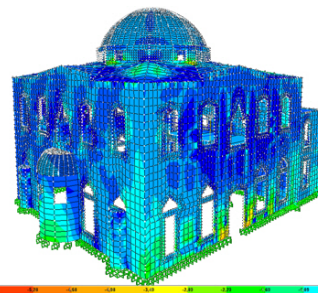


Fig. 42 Vertical normal stresses (in MPa) for the retrofitted Church by applying mass impregnation, subjected to Santa Tecla strong ground motion accelerogram

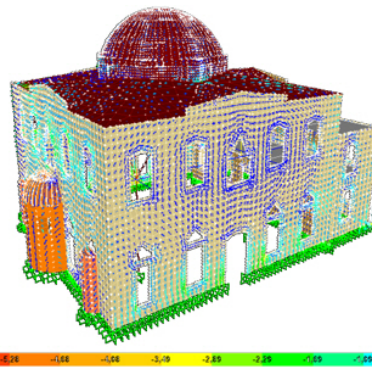


Fig. 43 Direction of stresses for the case of the fixed-base Church subjected to Observatorio strong ground motion accelerogram

conjunction with mass impregnation is shown next for the case of Santa Tecla strong ground motion accelerogram with expectation that these tensile failures will eventually diminish and exhibit a local character. Indeed, for the case of modulus of elasticity equal to 7.08 GPa and

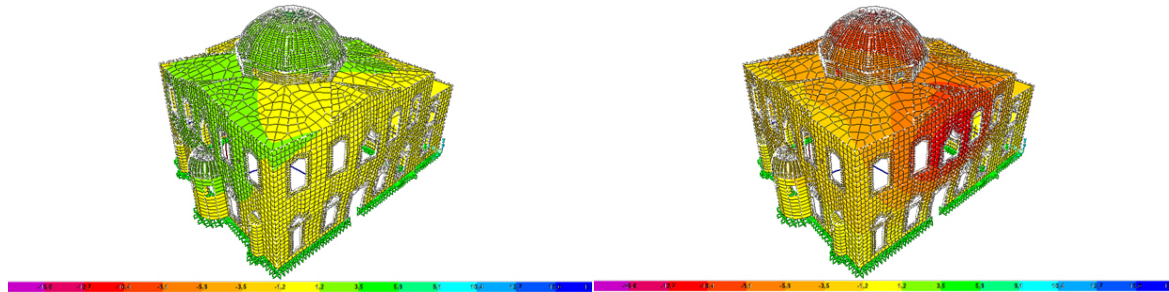


Fig. 44 Horizontal displacements along the X direction of the retrofitted Church by applying mass impregnation and jacketing, subjected to Santa Tecla strong ground motion accelerogram

Fig. 45 Horizontal displacements along the Y direction of the retrofitted Church by applying mass impregnation and jacketing, subjected to Santa Tecla strong ground motion accelerogram

damping ratio equal to 4%, Figs. 41 and 42 show a favorable distribution for both horizontal and vertical normal stresses of the retrofitted fixed-based Church. Tensile failures are localized at the external sides of peripheral walls. To get an idea of the direction of total stresses, Fig. 43 is provided for interpretation purposes of the stress results of Figs. 41 and 42. Similar results can be obtained for all cases when taking into account SSI effects.

Finally, Figs. 44 and 45 show the horizontal displacements at both X and Y directions of the retrofitted fixed-based Church when subjected to the Santa Tecla accelerograms. A comparison between Figs. 35 and 44 and Figs. 36 and 45, reveals that the proposed retrofit is also efficient in reducing seismic displacements.

5. Conclusions

Restoration and retrofitting of masonry monumental structures in Greece constitutes a special technical challenge due to the frequent occurrence of earthquakes. In this work, the seismic response and retrofit proposals of the St. Titus Church have been studied in detail using response spectrum and linear time-history analyses. These linear analyses have been performed for a preliminary seismic response assessment of the Church. The main conclusions are the following:

1) Taking into account different values of modulus of elasticity and modal damping ratio for masonry as well as considering or no SSI effects, response spectrum analyses according to Eurocode 8 (2009) reveal that the Church is expected to exhibit extensive tensile failures at the external sides of the peripheral walls as well as compressive failures among the openings of the peripheral walls. The compressive failures can be reduced if the mechanical properties of masonry are improved.

2) The expected failures are in accordance with the damage observed to the external sides of the Church before its restoration in the decade 1970-1980 as well as with the current damage state of the external sides.

3) Seismic retrofit of the structure by using mass impregnation almost eliminates compressive failures and reduces the extent of tensile ones. Application of mass impregnation in conjunction with reinforced concrete jackets at the internal part of the peripheral masonry walls and at the walls between the main temple and the vestibule, leads to only few tensile failures of local

character.

4) Similar results regarding failures have been found by performing linear time-history analyses of the structure by using recorded accelerograms that satisfy the restrictions of Eurocode 8 (2009). Seismic retrofit of the Church by using mass impregnation in conjunction with reinforced concrete jackets has been also supported by linear time-history analyses and lead to an increase of the seismic resistance of the Church as only few tensile failures of local character are expected to occur.

Acknowledgments

The authors would like to thank the 13th Ephorate of Byzantine Antiquities for providing the detailed architectural drawings, originally imprinted by N. Kritsotakis, as well as useful historical data regarding the construction and conservation of the St. Titus Church.

References

- Arêde, A., Costa, A., Moreira, D. and Neves, N. (2012), "Seismic analysis and strengthening of Pico Island Churches", *Bull. Earthq. Eng.*, **10**(1), 181-209.
- Arvanitaki, A. and Voyadjis, S. (2012), "The Pantokrator Gate of the Venetian walls of Heracleion, Krete", *Proceedings of the 3rd Pan-Hellenic Conference on Restoration*, Athens, Greece.
- Beskos, D.E. (1993), "Use of finite and boundary elements in the analysis of monuments and special structures", *Bull. Greek Assoc. Civ. Eng. Greece*, **216**, 31-43. (in Greek)
- Beskos, D.E. (1994), "Use of finite and boundary elements in the analysis of monuments and special structures", *Bull. Greek Assoc. Civ. Eng. Greece*, **217**, 15-32. (in Greek)
- Betti, M. and Galano, L. (2012), "Seismic analysis of historic masonry buildings: The Vicarious Palace in Pescia (Italy)", *Buildings*, **2**(2), 63-82.
- Betti, M., Bartoli, G. and Orlando, M. (2010), "Evaluation study on structural fault of a Renaissance Italian palace", *Eng. Struct.*, **32**(7), 1801-1813.
- Bull, J.W. (2001), *Computational modeling of masonry, brickwork and blockwork structures*, Saxe-Coburg Publications, Stirling, United Kingdom.
- COSMOS (1999), *Consortium of Organizations for Strong-Motion Observation Systems - Strong motion virtual data center (VDC)*, <http://www.strongmotioncenter.org/vdc/scripts/earthquakes.plx>.
- EC6 (2009), *Eurocode 6 - Design of masonry structures, Part 1-1: General rules for reinforced and unreinforced masonry structures*, European Committee for Standardization (CEN), Brussels.
- EC8 (2009), *Eurocode 8 - Design of structures for earthquake resistance, Part 1: General rules, seismic actions and rules for buildings*, European Committee for Standardization (CEN), Brussels.
- Elmenschawi, A., Sorour, M., Mufti, A., Jaeger, L. and Shrive, N. (2010), "Damping mechanisms and damping ratios in vibrating unreinforced stone masonry", *Eng. Struct.*, **32**(10), 3269-3278.
- Kržan, M., Gostič, S., Cattari, S. and Bosiljkov, V. (2015), "Acquiring reference parameters of masonry for the structural performance analysis of historical buildings", *Bull. Earthq. Eng.*, **13**(1), 203-236.
- Meli, R. and Peña, F. (2004), "On elastic models for evaluation of the seismic vulnerability of masonry churches", *Structural analysis of historical constructions*, eds., Modena, Lourenço and Roca, 1121-1131, Taylor and Francis, London.
- Modena, C., Zavarise, G. and Valluzzi, M.R. (1997), "Modelling of stone masonry walls strengthened by RC jackets", *Proceedings of the 4th International Symposium on Computer Methods in Structural Masonry*, 285-292, Florence, Italy.
- Mulliken S. and Karabalis, D.L. (1998), "Discrete model for dynamic through-the-soil coupling of 3-D

- foundations and structures”, *Earthq. Eng. Struct. Dyn.*, **27**(7), 687-710.
- Pagnini, L.C., Vicente R., Lagomarsino, S. and Varum, H. (2011), “A mechanical model for the seismic vulnerability assessment of old masonry buildings”, *Earthq. Struct.*, **2**(1), 25-42.
- Papazachos, V.K. and Papazachou, K. (2004), *The earthquakes of Greece*, Ziti Publications, Thessaloniki, Greece.
- Penazzi, D., Valluzzi, M.R., Saisi, A., Binda, L. and Modena, C. (2001), “Repair and strengthening of historic masonry buildings in seismic areas”, *Proceedings of the International Congress: More than two thousand years in the history of architecture safeguarding the structure of our architectural heritage*, 1-6, Bethlehem, Palestine.
- Roca, P., González, J.L., Marí, A.R. and Oñate, E. (1997), *Structural analysis of historical constructions, - Possibilities of numerical and experimental techniques*, Barcelona, Spain.
- SAP 2000 (2010), *Static and Dynamic Finite Element Analysis of Structures*, Version 14.2.0, Computers and Structures, Berkeley, California, USA.
- Tomaževič, M and Apih, V. (1993), “The strengthening of stone masonry walls by injecting the masonry friendly grouts”, *Eur. Earthq. Eng.*, **7**, 10-20, Patron, Bologna, Italy.
- Tomaževič, M. (1999), *Earthquake-Resistant design of masonry buildings*, Imperial College Press, London.
- Triantafyllou, T.C. and Fardis, M.N. (1997), “Strengthening of historic masonry structures with composite materials”, *Mater. Struct.*, **30**(8), 486-496.
- Tsapanos, T.M. (2003), “A seismic hazard scenario for the main cities of Crete island, Greece”, *Geophys. J. Int.*, **153**(2), 403-408.
- Vasilakis, M., Vasilakis, N. and Papadrakakis, M. (1979), *Report on the static behavior of the St. Titus dome*, Report in Greek submitted to the Technical Chamber of Greece, Heraklion, Crete, Greece.